

# THE ANTENNA LABORATORY

## RESEARCH ACTIVITIES in ---

*Automatic Controls    Antennas    Echo Area Studies*  
*Microwave Circuits    Astronautics    E M Field Theory*  
*Terrain Investigations    Radomes    Systems Analysis*  
*Wave Propagation    Submillimeter Applications*

N65 13274

(ACCESSION NUMBER)

32

(PAGES)

0059912

(NASA CR OR TMX OR AD NUMBER)

(THRU)

(CODE)

17

(CATEGORY)

### The Static Response Characteristics of a Carbon Bolometer Element

by

Glean G. Shephard

Grant Number NaG-74-60

15 October 1964

Prepared for:

National Aeronautics and Space Administration  
1520 H Street Northwest  
Washington 25, D.C.

Department of ELECTRICAL ENGINEERING



THE OHIO STATE UNIVERSITY  
RESEARCH FOUNDATION  
Columbus, Ohio

GPO PRICE \$

OTS PRICE(S) \$

Hard copy (HC) \$

Microfiche (MF) \$

2.00

.50

REPORT

by

THE OHIO STATE UNIVERSITY RESEARCH FOUNDATION  
COLUMBUS, OHIO 43212

Sponsor            National Aeronautics and Space Administration  
                    1520 H Street Northwest  
                    Washington 25, D.C.

Grant Number      NsG-74-60

Investigation of   Receiver Techniques and Detectors for Use at  
                         Millimeter and Submillimeter Wave Lengths

Subject of Report   The Static Response Characteristics of a Carbon  
                         Bolometer Element

Submitted by       Glenn G. Shephard  
                         Antenna Laboratory  
                         Department of Electrical Engineering

Date                15 October 1964

The material contained in this report is also used as a thesis submitted to the Department of Electrical Engineering, The Ohio State University as partial fulfillment for the degree Master of Science.

## ABSTRACT

13274

The electrical resistivity of carbon resistor material has been experimentally determined as a function of temperature and has been used to calculate the static response characteristics of a particular carbon bolometer element without making use of the usual isothermality and constant thermal conductivity assumptions.

*author*

## CONTENTS

Chapter		Page
I	INTRODUCTION.....	1
II	THE MATERIAL PROPERTIES.....	3
	The electrical resistivity.....	3
	Experimental determination of electrical resistivity.....	6
	The thermal conductivity.....	13
III	DEVELOPMENT OF THE RESPONSE CHARACTERISTICS.....	14
IV	CONCLUSIONS.....	20
APPENDIX		
I	STRUCTURE OF THE CARBON COMPOSITION RESISTOR MATERIAL.....	23
II	THERMAL CONDUCTIVITY OF CARBON COMPOSITION RESISTOR MATERIAL.....	25
	BIBLIOGRAPHY.....	27

## CHAPTER I INTRODUCTION

A prerequisite to proper understanding of thermal, bolometer type, detection systems is knowledge of the static input-output characteristics (i. e., power input versus electrical signal output) of the various bolometer material elements. The purpose of this report is to provide this information for a carbon bolometer element fabricated in a particular physically realizable geometry. These characteristics will then provide a basis for the future analysis of a carbon bolometer detection system.

The term "carbon bolometer" is a gross misnomer. The material used to make carbon bolometers is really carbon composition resistor material; a mixture of some form of carbon or graphite, filler material, and binder material[ 1]. The complexity of this mixture, illustrated in Appendix I, precludes derivation of the required material parameters (such as the electrical resistivity) from a theoretical basis. Consequently these have been experimentally determined (first and second hand) and presented in Chapter II.

In Chapter III the experimentally determined electrical resistivity and thermal conductivity, of resistor material, have been used to calculate the response (i. e., input-output) characteristics. The analysis consists primarily of the numerical solution, using a Runge-Kutta[ 2] method, of the nonlinear differential heat equation in the material.

The result of this analysis is the static characteristics, i. e., the dc output voltage as a function of the input power.

## CHAPTER II

### THE MATERIAL PROPERTIES

Analysis of the resistor material element requires knowledge of the functional relationships with temperature of two parameters: the electrical resistivity and the thermal conductivity. The object of this chapter is to present the temperature dependencies of these two parameters and to provide their justifications by means of experimental results obtained here and elsewhere.

#### The Electrical Resistivity

The electrical resistivity of resistor material has not, to the author's knowledge, been published. Several papers do, however, illumine the problem. Clement-Quinnell[ 3] and Templeton-MacDonald[ 4] both discuss carbon resistor resistance variation with temperature while Mrozowski [ 5] deals with the polycrystalline graphite resistivity-temperature dependence.\* None however, specifically

---

\* As background material the following articles re monocrystalline and polycrystalline graphite should be of interest:

P. R. Wallace, Phys. Rev., 71, 622 (1947)  
D. Bowen, Phys. Rev., 76, 1878 (1949)  
E. E. Loebner, Phys. Rev., 102, 46 (1956).

formulate the carbon composition material resistivity-temperature dependence. What they can offer to the problem is discussed below.

Clement and Quinnell, following detailed measurements on Allen Bradley resistors, posed the following equation as descriptive of resistance variation with temperature below  $20^{\circ}\text{K}$ :

$$(1) \quad \log R + K'/\log R = A' + B'/T .$$

At low temperatures the term  $K'/\log R$  is of decreasing importance and, if we do not demand extreme exactitude, the equation may be approximated as  $R = A \exp(K/T) = A \exp(\Delta E/kT)$  where for a 56 ohm resistor  $\Delta E = 7 \times 10^{-4} \text{ eV}$  which corresponds in form to the findings of Templeton and MacDonald in their work on Erie resistors.\* From this, it seems probable that all carbon composition resistors have the common resistance-temperature characterization

$$(2) \quad R = A \exp(K/T) \quad \text{ohms}$$

below  $20^{\circ}\text{K}$ . However, the existence of a direct correlation in form between this exponential resistance-temperature dependence and the material resistivity-temperature dependence is not certain. As both

---

\* The "activation energy",  $\Delta E$ , described and discussed by Templeton and MacDonald was of an order of magnitude, or so, lower than that found by Clement and Quinnell with Allen Bradley resistors (their  $\Delta E \sim 10^{-5} \text{ eV}$ ).



the electrical resistivity and the thermal conductivity are temperature dependent to see such direct correlation is to either see an essential isothermality throughout the resistor or to assume the effects of the existent temperature variations as negligible. Yet Berman[ 6] indicates in his paper that a gradient of  $1/10 \text{ K}^0$  may exist in a resistor at  $2^0\text{K}$ . This along with the fact that his published thermal conductivity for resistor material (as  $\sim T^2$ ) differs significantly from the resistor thermal conductance reported by Clement and Quinell (as  $T$ ) raises grave doubts as to the truth of such correlation.

Mrozowski's paper deals entirely with polycrystalline graphite and as such his results and conclusions can only be tenuously related, in a qualitative manner, to the composition resistor material question. His polycrystalline graphite resistivity-temperature curves indicate, as did Clement and Quinell's and Templeton and MacDonald's, that the resistivity of resistor material increases sharply with decrease in temperature (at low temperatures, i. e.,  $1^0\text{-}4^0\text{K}$ ) without, however, giving any indication of functional form. This ambiguity in the low temperature resistivity-temperature dependence prompted the following experiment to determine this resistivity form.

## Experimental Determination of Electrical Resistivity

A 100 ohm, one watt, Allen Bradley carbon composition resistor was used for a thermometer after the manner of Clement and Quinell. The insulation was removed to reduce the heat capacity and to improve the thermal contact with surroundings. 56 ohm, two watt resistors were used to fabricate five elements of varying thickness,  $\omega$ , as shown in Figure 1. Nickel contacts were electrodeposited on opposite (thin)

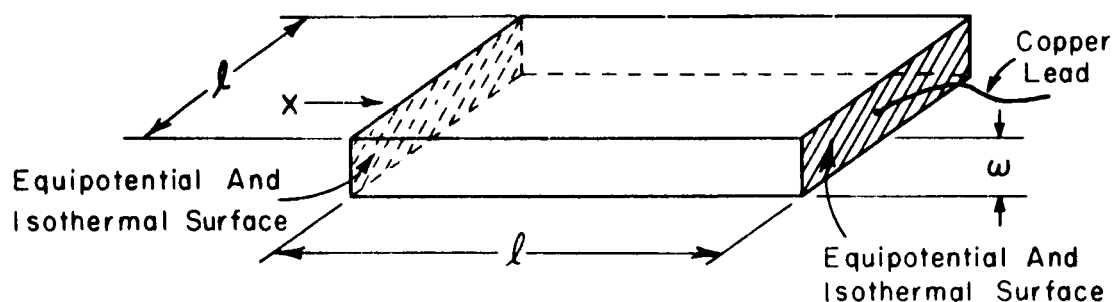


Fig. 1--The carbon element.

end surfaces and copper leads were soldered to them. These contacts proved ohmic at liquid helium temperatures. The thicknesses of the elements ranged from 0.0305 cm to 0.0635 cm and this extreme thinness, coupled with complete thermal contact with the sink on all surfaces justified the isothermal assumption which produced geometric transformation between resistance measured and resistivity; i. e., (resistivity) = (resistance)(cross-section area normal to current flow)/(length of current path).

Measurements were taken in the following manner. The thermometer and two elements were placed in a glass double-dewar cryogenic system - unshielded from the cryogenic fluid. Liquid helium was added and pumped with a roughing pump to lower the system temperature. The pumping apparatus is shown in Figure 2. After reaching  $\sim 1.4^{\circ}\text{K}$ , pumping was discontinued causing the cryogenic system to reheat. Simultaneous measurements of element and thermometer resistance were taken during this warm-up period. A photograph of the entire experimental assembly is shown in Figure 3. Figure 4 illustrates the measurement methods. The discontinuity in the resistance-temperature plot noted by Clement and Quinell (due primarily to the helium II penetration of the carbon material below the Lambda point) at the Lambda point, for immersed carbon material, was observed providing one thermometer calibration point. The other calibration point obtained was at atmospheric pressure, i. e.,  $4.2^{\circ}\text{K}$ . As the equations of Clement and Quinell could not be made to fit the two known points of the thermometer curve, the exponential approximation of Eq. (2) was used to provide the temperature calibration curve.

Next, to remove the helium penetration discontinuity, a vacuum-tight brass chamber was constructed to hold both the elements and the



Fig. 2--The pumping apparatus.



Fig. 3--The experimental assembly.

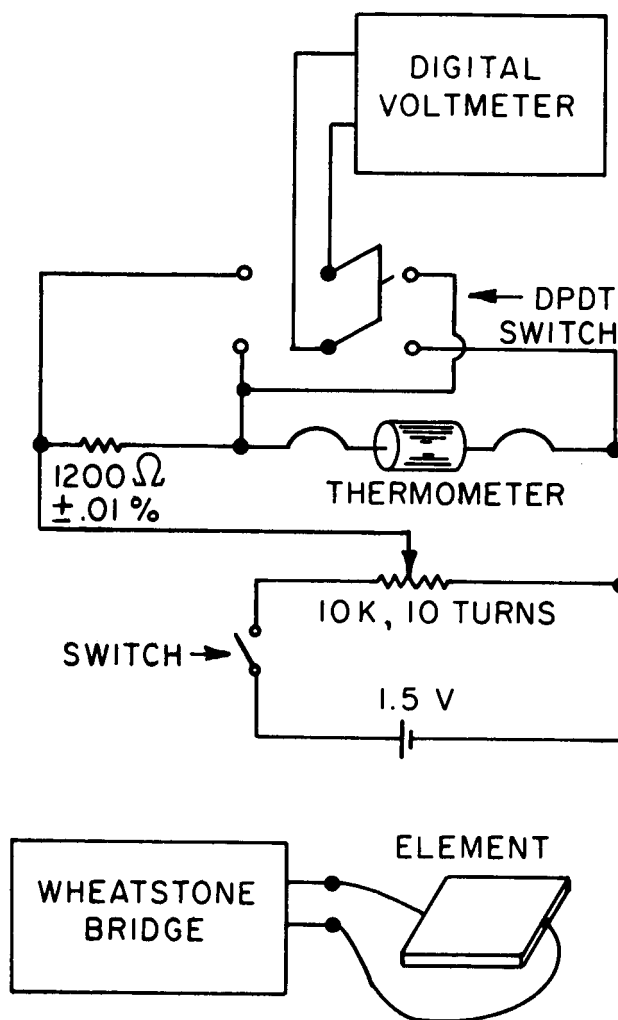


Fig. 4--The measurement methods.

thermometer. G.E. 7031 varnish was used for the low temperature glue to provide electrical insulation and thermal conduction from and with the container. Both surfaces of the element were glued directly to a chamber surface. The vacuum-tight seal was provided by an indium "O" ring seal between two lapped chamber surfaces. The entire assembly is shown in Figure 5.

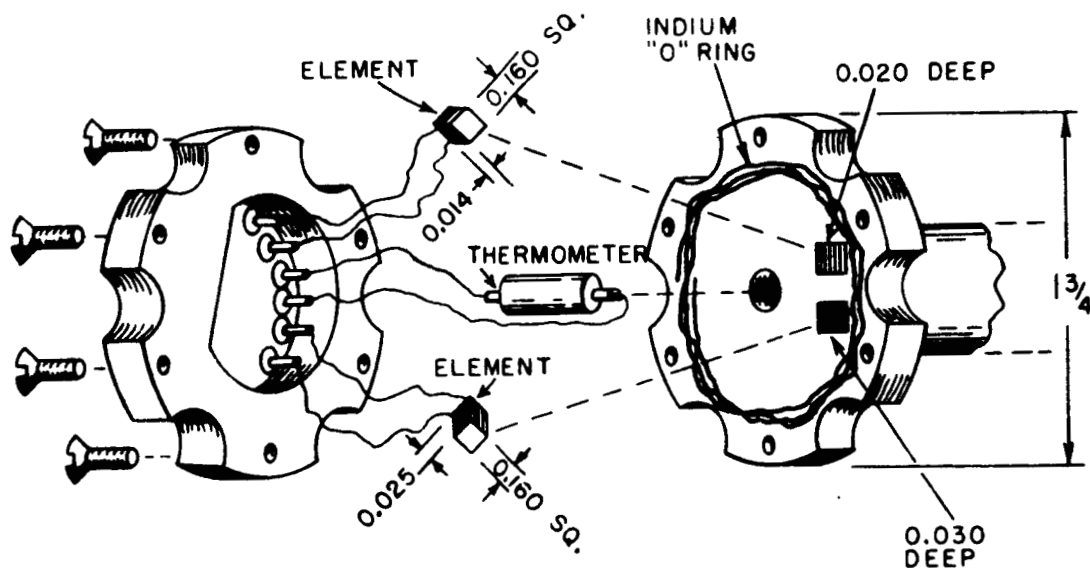


Fig. 5--Vacuum-tight element and thermometer container for resistivity determination.

Measurements of element and thermometer resistance were again taken, as described previously, and the resultant experimental resistivity-temperature plot is shown in Figure 6. Comparison of the Clement and Quinell resistance curve (for a 56 ohm resistor) with the resistivity curve reveals an essential parallelism, Figure 7, which definitely points to an identity of form; i. e., they both vary as

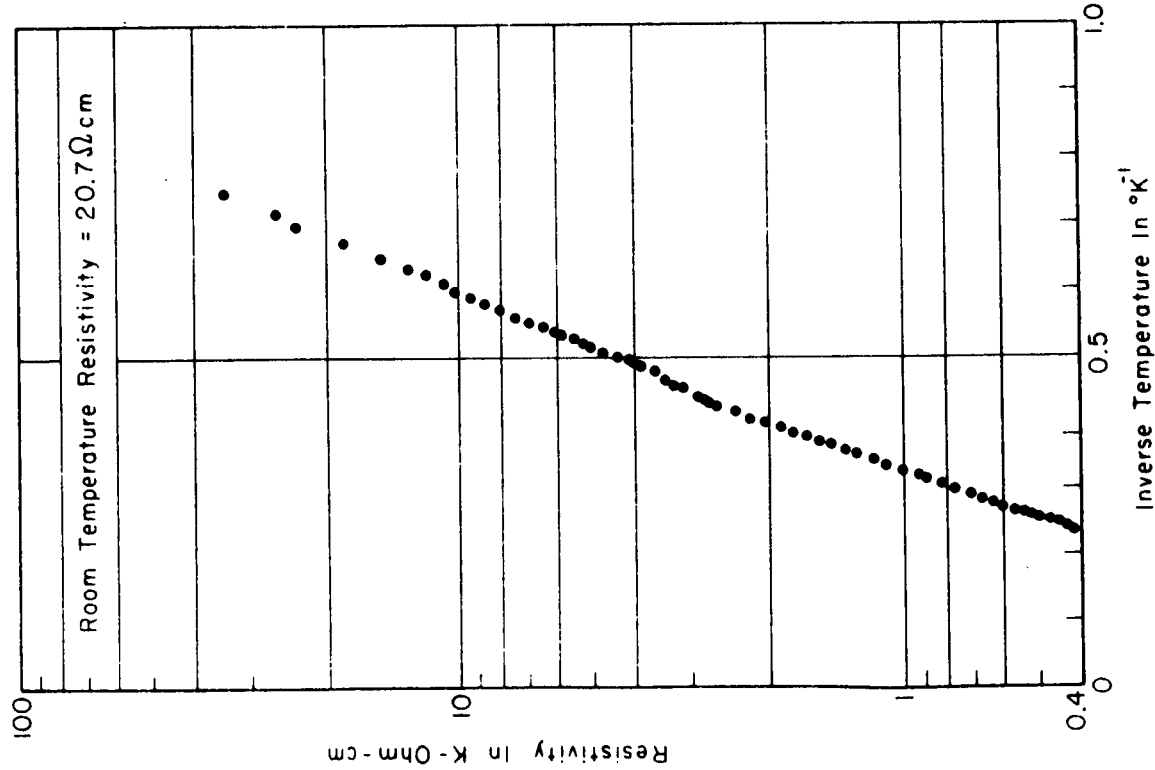


Fig. 6--Resistivity-temperature characteristic of 56 ohm(nom.) Allen-Bradley carbon composition material.

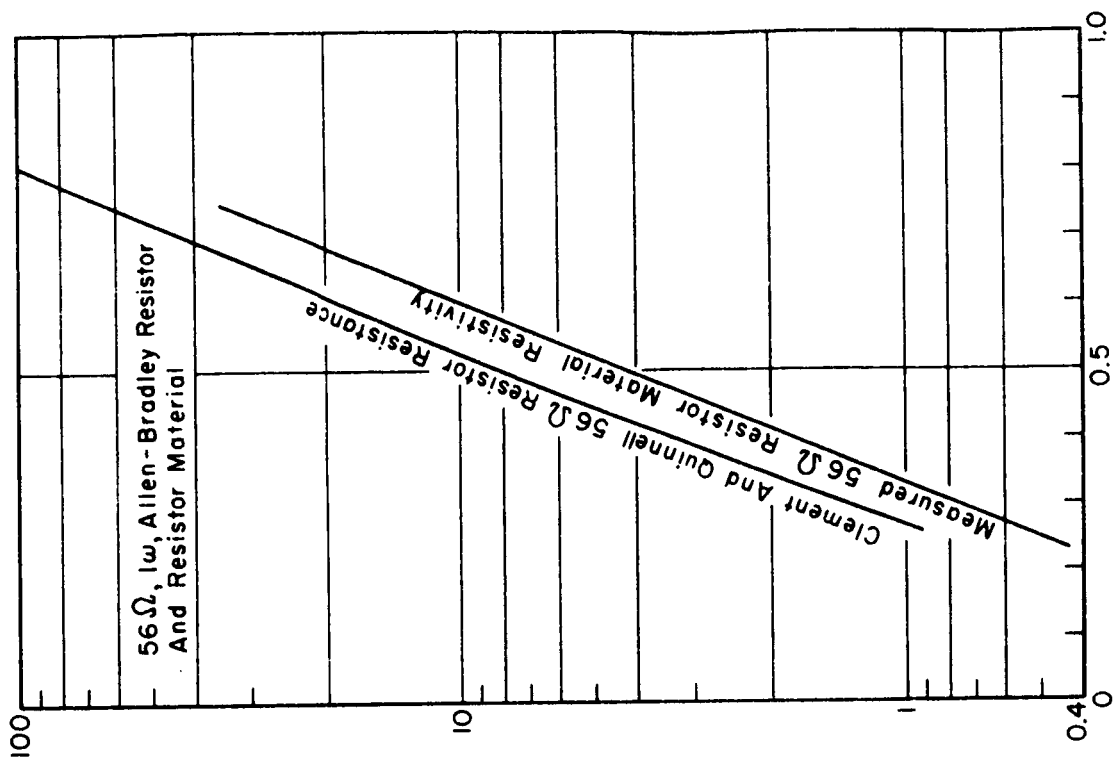


Fig. 7--Comparison of the Clement and Quinell resistor resistance curve with the measured resistivity curve.



Eq. (2) with identical  $K$ 's. Thus the resistance-temperature dependence of Clement and Quinell is confirmed as being representative of the resistivity-temperature variation. That is, the effects of the temperature gradients in the resistor are shown to be negligible.

The resistivity-temperature dependence that will be used in the development of the next chapter will be that measured experimentally, Figure 6,

$$(3) \quad \rho(T) = 61.4 \exp(8.52/T) \quad \text{ohms} \quad .$$

#### The Thermal Conductivity

Turning to the thermal conductivity we find none of the problems which arose with the electrical resistivity. Berman[ 6] plots the thermal conductivity of resistor material versus temperature and from this curve the following relation is drawn and used (Appendix II).

$$(4) \quad K(T) = 10^{-5} T^2 \quad \text{watt/cm/deg} \quad .$$

### CHAPTER III

#### DEVELOPMENT OF THE RESPONSE CHARACTERISTICS

The static response characteristics that are sought are those relating absorbed radiant power to resultant output voltage. The carbon element that shall be analyzed is pictured in Figure 1. Maintaining sink temperature only on the electrical contact surfaces allows simplification of the problem treated to that of one dimension. The assumption made in this simplification is isothermality of material cross-sections normal to current flow direction. This assumption neglects effects of re-radiation and assumes uniform absorption of radiant power throughout the element. A further assumption made, in the name of simplicity, is that of constant current flow for all resistance variations.

The development has the following outline. First, as heat is generated through all the element and exits only through the end contacts, the temperature distribution along the element is determined. Then, the total, overall element resistance is obtained by an integration of the resistivity. Because of the constant current

assumption the resultant voltage is simply the current-resistance product. Finally, isothermals are drawn on element resistance-sink temperature curves (drawn for different power levels) and the requisite response curves result.

The general heat equation in the carbon element may be written as

$$(5) \quad \nabla \cdot K(T) \nabla T + q(T) = C(T) W \partial T / \partial t$$

where  $K(T)$  = thermal conductivity (watt/deg/cm)

$T$  = temperature ( $^{\circ}\text{K}$ )

$q(T)$  = internally generated heat (watts)

$C(T)$  = specific heat

$W$  = specific weight

$t$  = time .

For the static case,  $\partial T / \partial t = 0$ , and the general equation may be written

$$(6) \quad \nabla \cdot K(T) \nabla T + q(T) = 0 \quad .$$

Simplifying further to the one dimensional case (in  $X$ ) the equation, descriptive of the present problem, becomes

$$(7) \quad d/dX(K(T) dT/dX) + q(T) = 0 \quad .$$

The internally generated heat consists of  $\bar{J} \cdot \bar{E}$  losses of the bias current and the absorbed radiative power. Thus

$$(8) \quad q(T) = \bar{J} \cdot \bar{E} + p$$

The carbon material is isotropic in bulk and therefore  $\bar{J}$  and  $\bar{E}$  are coincident causing  $\bar{J} = \sigma \bar{E}$  or  $\bar{E} = \rho \bar{J}$ . Making use of the constant current approximation and the isothermality assumption (transverse to X) allows us to write for the element of Figure 1

$$\bar{J} \cdot \bar{E} = |\bar{J}|^2 \rho(T) = (I^2 / l^2 \omega^2) \rho(T)$$

and

$$(9) \quad q(T) = (I^2 / l^2 \omega^2) \rho(T) + p$$

From Chapter I we have

$$(4) \quad K(T) = 10^{-5} T^2 = LT^2$$

and

$$(3) \quad \rho(T) = 61.4 \exp(8.52/T) = B \exp(K/T)$$

Upon substitution, the heat equation becomes

$$(10) \quad d/dX(LT^2 dT/dX) + (I^2 B / l^2 \omega^2) \exp(K/T) + p = 0$$

where  $p = (\text{total absorbed power})/(\text{element volume})$ . This equation is solved by numerical integration for the following boundary conditions:

$$X = 0; T = T_{\max}, dT/dX = 0$$

$$X = \pm l/2; T = T_0 .$$

Having obtained the temperature distribution along the element, the overall element resistance is found by integration over  $X$  from  $-l/2$  to  $+l/2$ ;

$$(11) \quad R = (1/l\omega) \int_{-l/2}^{+l/2} \rho(T) dX = (2B/l\omega) \int_0^{l/2} \exp(K/T) dX .$$

Curves of overall resistance,  $R$ , are then plotted versus sink or end temperature for different radiant power levels (constant bias current) and from this the response characteristics are derived.

The actual numerical values used include of course the specific parameters presented in Chapter I. The physical dimensions are those of the experimental element; i. e.,  $l = 0.407$  cm and  $\omega = 0.0356$  cm. A bias current of 5 microamperes was chosen as not creating excessive dissipation and being controllable and measurable.

Absorbed radiant power levels were chosen in  $10^{-6}$  watt units ranging from 0 watt to  $9 \times 10^{-6}$  watt producing the readily 'drawable' curves of Figure 8. Isothermals were constructed from 1.2°K to 2.2°K in 0.2K° steps and the response characteristics drawn in these values are shown in Figure 9.

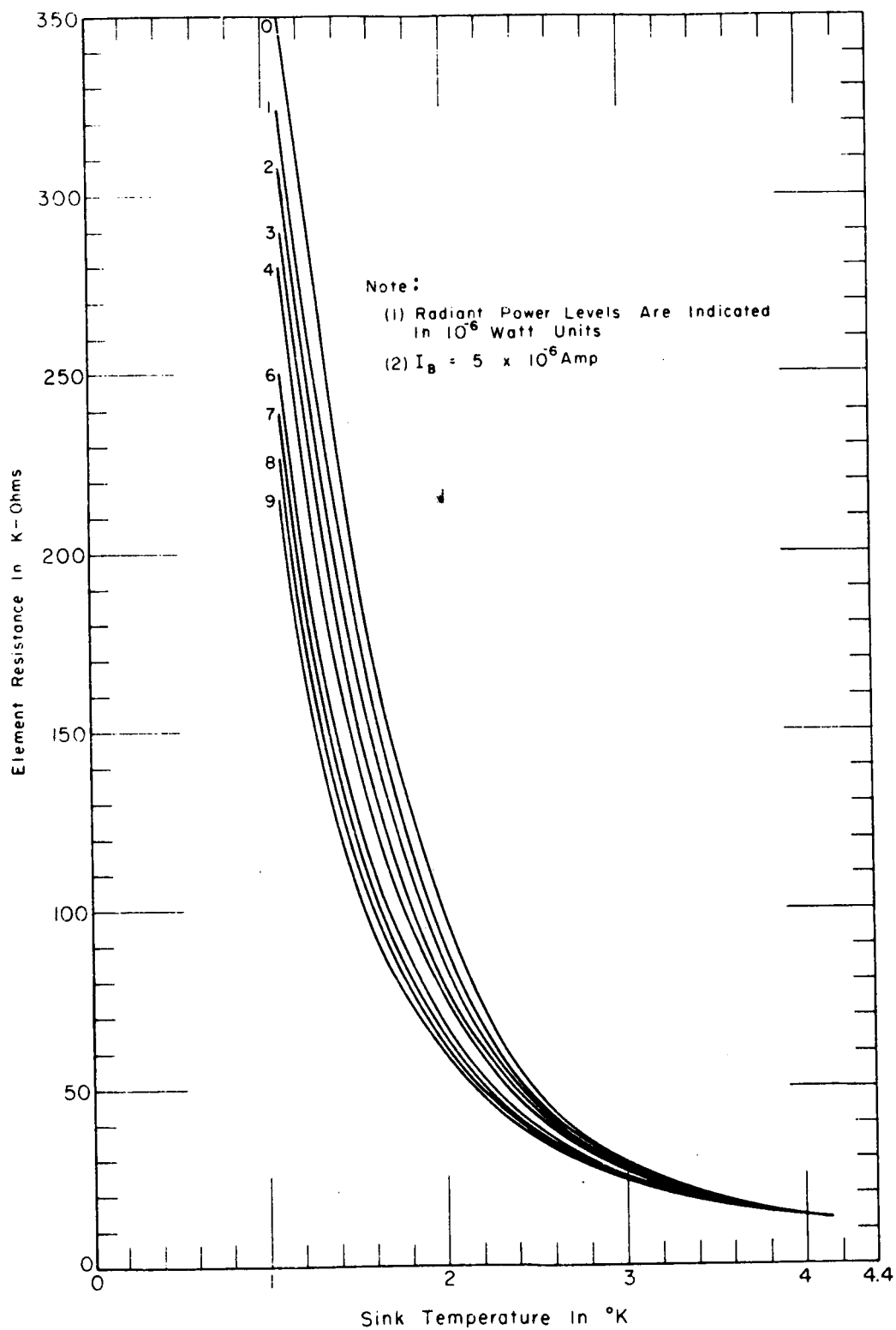


Fig. 8--Overall element resistance-sink temperature curves for different absorbed radiant power levels.

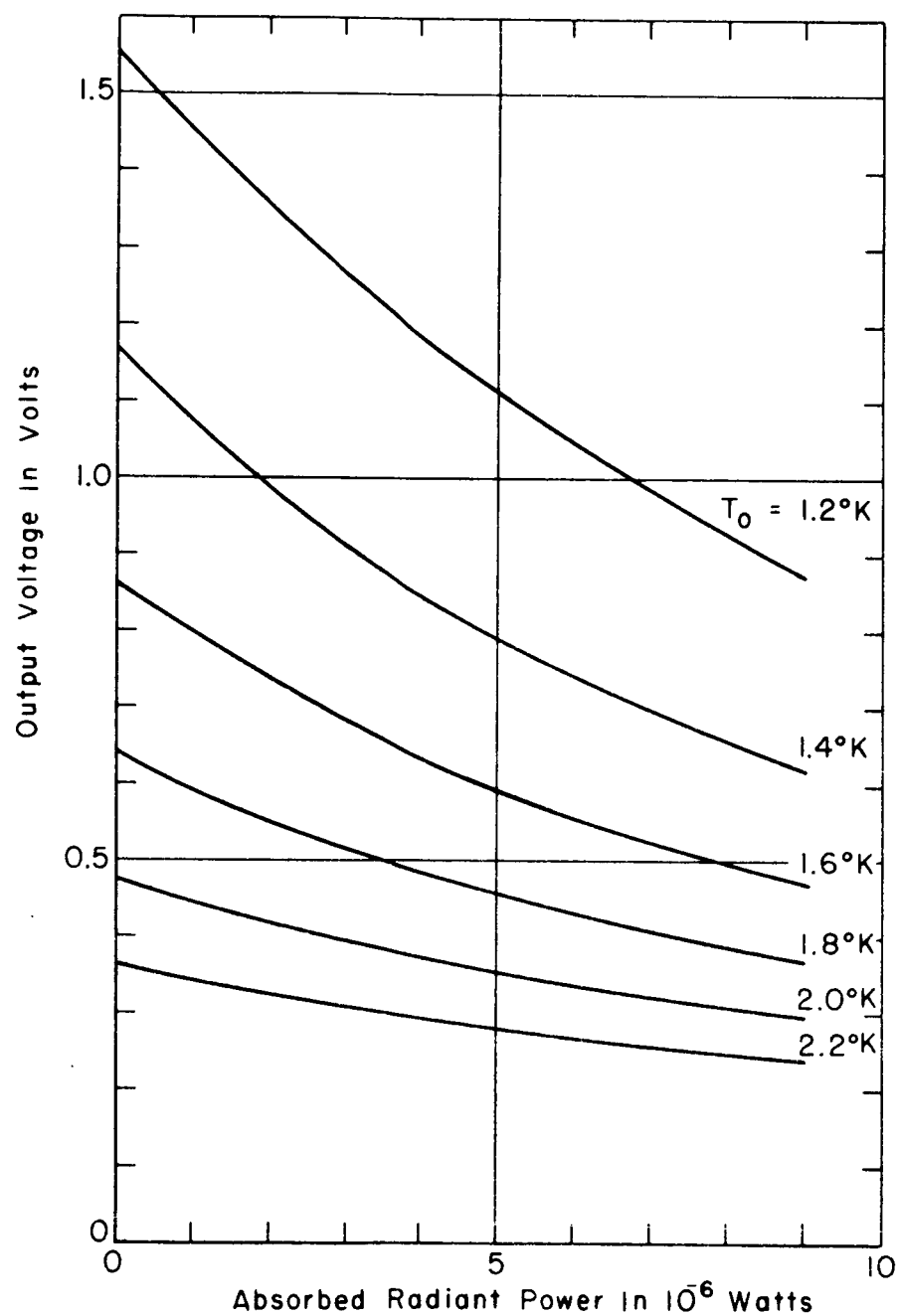


Fig. 9--Static response characteristics  
for the carbon bolometer element.

## CHAPTER IV

### CONCLUSIONS

From the experimental data and the analysis, the following conclusions may be drawn.

1. The resistivity of carbon resistor material varies as  $B \exp(K/T)$  which is in direct correspondence with resistor resistance temperature dependence given by existing data. This evidences the negligibility of the temperature variation effects within the carbon resistor.
2. Using the experimental resistivity data the static characteristics of a particular carbon bolometer element were calculated without making the usual isothermality and constant thermal conductivity assumptions.
3. Plotting the slopes of the response curves at  $P = 0$  versus temperature yields an ultimate responsivity-temperature characteristic applicable to very low power levels. This curve is plotted in Figure 10. Taking a value, from the curve, of  $2.8 \times 10^4$  volts per watt at  $2.1^\circ\text{K}$  it is seen to compare very favorably with the experimental carbon bolometer responsivity recorded by Putley[7] of  $2.1 \times 10^4$  volts per watt at  $2.1^\circ\text{K}$ . This



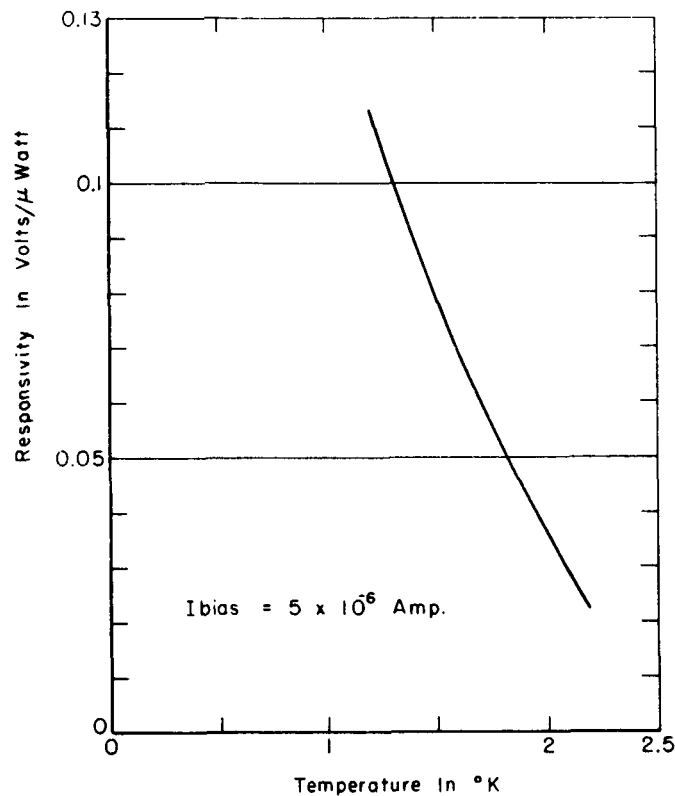


Fig. 10--Ultimate static responsivity of carbon bolometer element.

agreement can be regarded as a confirmation of the calculation.

4. An observation re the carbon bolometer is that its sensitivity is highly sink temperature dependent. The only way to refer to an optimum operating temperature is to define the lowest temperature attainable as the "optimum" operating temperature. This is a consequence of the nonlinearity of the element resistance-sink temperature curves. This sensitivity-temperature dependence adds a noise contribution which would be missing if the resistance curves were parallel and linear.

5. The similarity between these response characteristics (i.e., for the carbon element) and the usual radio tube characteristics is marked. Further work will be directed to development of small signal (a-c) characteristics in an analogous manner to the radio tube small signal analysis.

APPENDIX I  
STRUCTURE OF THE CARBON  
COMPOSITION RESISTOR MATERIAL

Initial work on the carbon resistor material element included the lapping and micrographing of a material sample. One of these micrographs is shown in Figure 11. The darker grey bodies were determined to be carbon or graphite by their nonsolubility in nitric acid (as indicated by the arrows) and the light grey areas the filler and binder. As may readily be noted, there is no ordering or symmetry in the structure. The separation of the carbon particles, one from another, is clearly evident illustrating markedly the variance of resistor material structure from that of polycrystalline graphite.

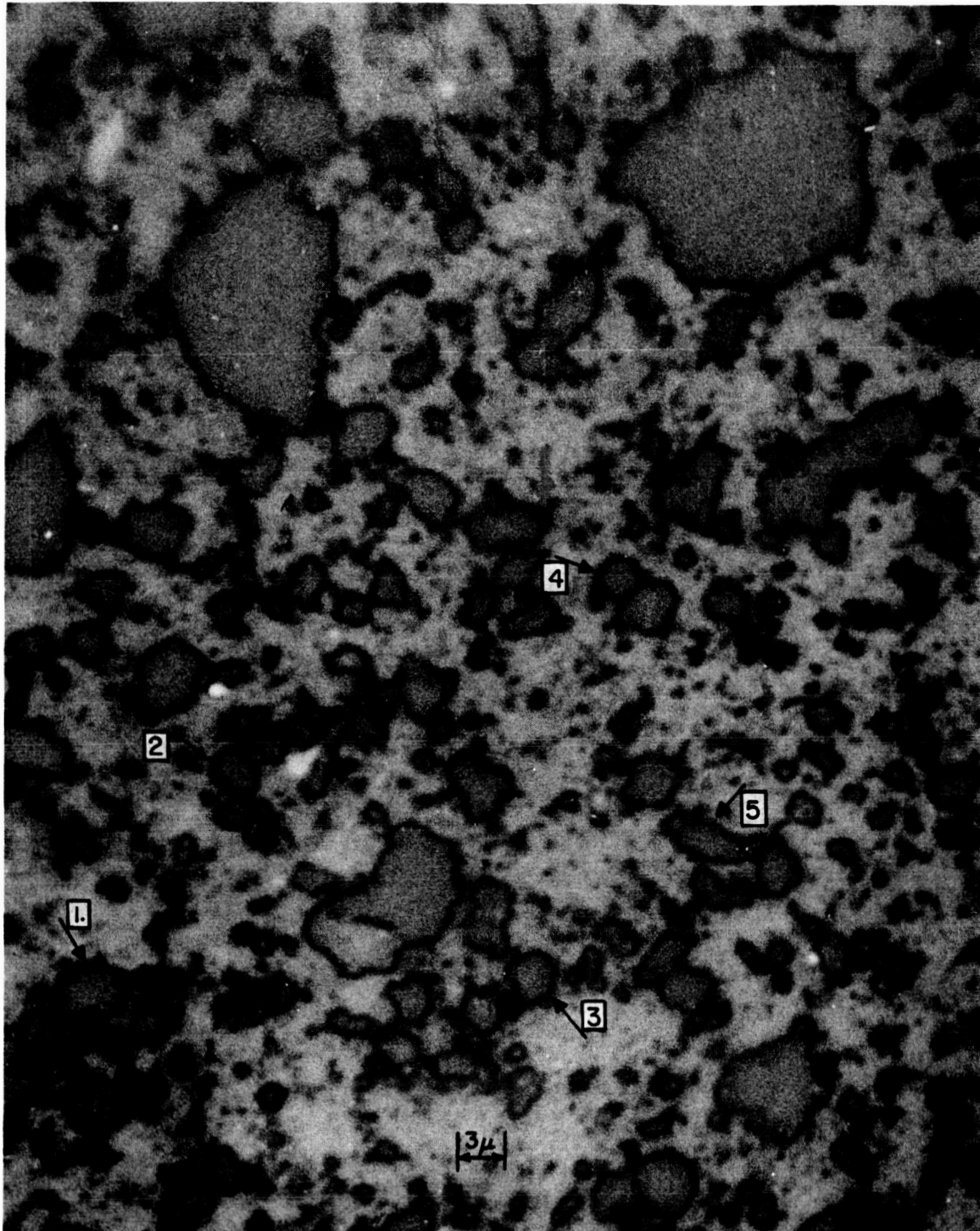


Fig. 11--Carbon resistor material structure.

APPENDIX II  
THERMAL CONDUCTIVITY OF CARBON  
COMPOSITION RESISTOR MATERIAL

In his paper Berman plots the experimentally determined thermal conductivity,  $\mathcal{K}(T)$ , of composition resistor material versus temperature. Figure 12 shows this plot and the manner in which the low temperature representation was obtained. From the slope of the curve and a point on it the actual relation is

$$\mathcal{K}(T) = (1.08 \times 10^{-5}) T^{1.87} \quad \text{watt/deg/cm} \quad .$$

Figure 13 shows a plot of  $T^2$  and  $T^{1.87}$  versus temperature over the range  $0^\circ\text{K}$  to  $4^\circ\text{K}$ . The degree to which  $T^2$  approximates  $T^{1.87}$  over this range of interest allows the following approximation for the thermal conductivity to be used for the development in Chapter II:

$$\mathcal{K}(T) = 10^{-5} T^2 \quad \text{watt/deg/cm} \quad .$$

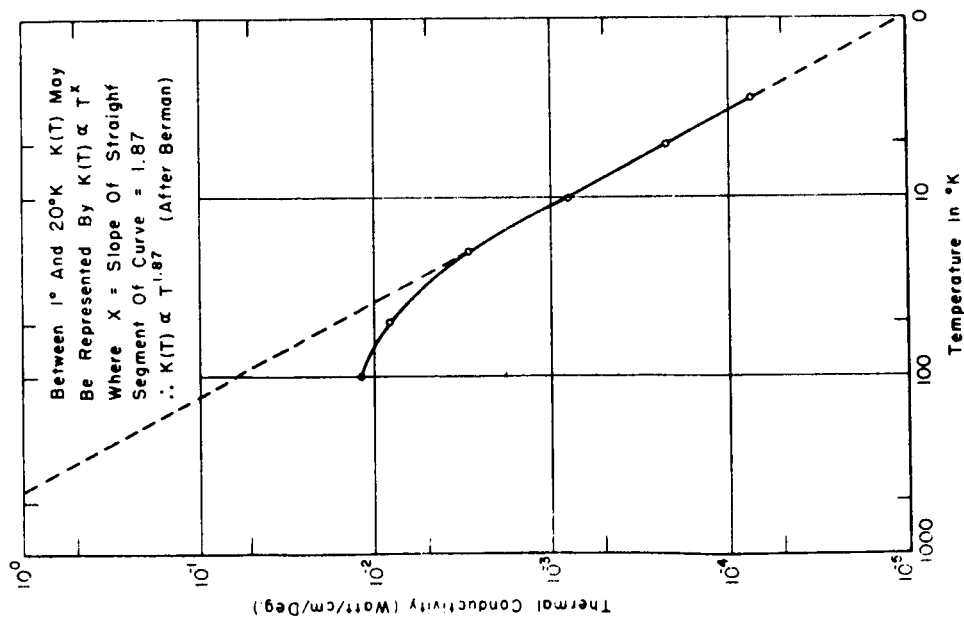


Fig. 12--Thermal conductivity of  
a carbon resistor.

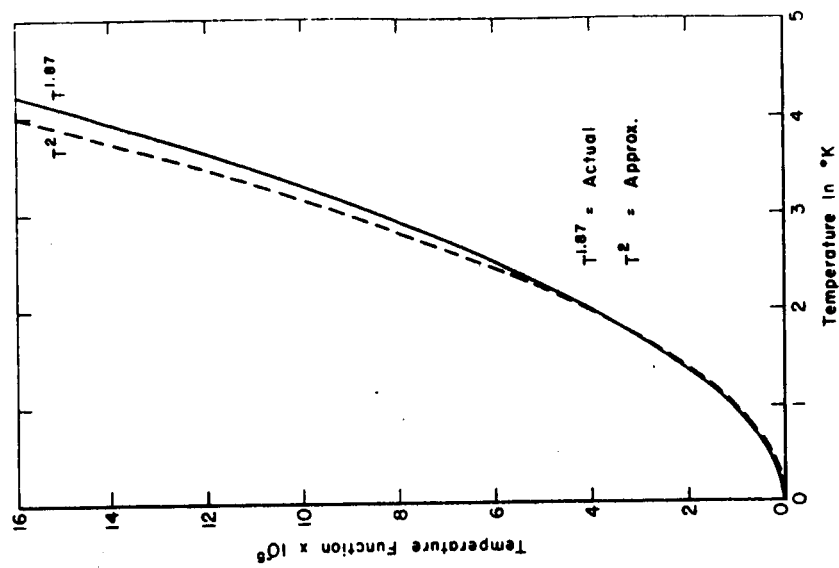


Fig. 13--Comparison of the temper-  
ature functions  $T^2$  and  $T^{1.87}$ .

## BIBLIOGRAPHY

1. Mantell, C.L., Industrial Carbon, D. Van Nostrand Company, Inc., New York, pp. 328-329, 1947.
2. Hildebrand, F.B., Introduction to Numerical Analysis, McGraw-Book Company, Inc., New York, pp. 233-239, 1956.
3. Clement, J.R. and Quinnell, E.H., "The Low Temperature Characteristics of Carbon-Composition Thermometers," Review of Scientific Instruments 23, No. 5, pp. 213-216, May 1952.
4. MacDonald, D.K.C. and Templeton, I.M., "The Electrical Conductivity and Current Noise of Carbon Resistors," Proceedings of the Physical Society (B) 66, pp. 680-687, 1953.
5. Mrozowski, S., "Semiconductivity and Diamagnetism of Polycrystalline Graphite and Condensed Ring Systems," Physical Review 85, No. 4, pp. 609-620, 1952.
6. Berman, R., "The Thermal Conductivity of Some Polycrystalline Solids at Low Temperatures," Proceedings of the Physical Society (A), 65, pp. 1038-1039, 1952.
7. Putley, E.H., "The Detection of Sub-MM Radiation," Proceedings of IEEE, 51, No. 11, p. 1421,